UDC 550.xx. + 55x.x/x.

Valerijs NIKULINS[1], Dmytro MALYTSKYY[2]

[1] SIA Geo Consultants, Olivu iela 9, Riga, LV-1004, Latvia, e-mail: seismolat@gmail.com, https://orcid.org/0000-0003-4489-8708
[2] Carpathian Branch of Subbotin Institute of Geophysics, National Academy of Sciences of Ukraine, email: dmalytskyy@gmail.com, https://orcid.org/0000-0002-9156-739X

https://doi.org/10.23939/jgd2023.02.053

PREDICTION OF SEISMIC IMPACTS AT THE SITE OF PLAVINU HPP FROM A POTENTIAL SEISMIC SOURCE IN KOKNESE (LATVIA)

The study considers the impact of seismic waves from the source of a potential earthquake in Latvia on the site of the Plavinu hydroelectric power station, which is located in unfavorable geological, tectonic, and geodynamic conditions. A direct seismology problem was solved in two stages to assess seismic impacts on the site. In the first stage, the modeling of synthetic seismograms was carried out, and in the second stage, a prediction of seismic impacts at the hydroelectric power station site was conducted. In the first stage, we used wave field modeling applying Green's method. In the second stage, ground motion characteristics were obtained using a one-dimensional, nonlinear ground response analysis method. A wave field of 15 Green's functions was obtained, which was then converted into a 3-component accelerogram. The accelerogram was then used as a seismic impulse to a Prequaternary sediment's surface. A set of engineering and seismic characteristics of soil was obtained, i.e. amplification, Fourier amplitudes, and spectral amplitudes. The paper demonstrates the ability to acquire valuable information about the seismic wave field and ground motion from macroseismic data from historical earthquakes. This is especially important for intra-plate conditions with limited seismic statistics. Prediction of engineering and seismic conditions are of great practical importance since they will allow us to identify the most vulnerable sites of the soil at the Plavinu HPP.

Key words: green functions; synthetic wave field; site response; amplification; Fourier amplitude; spectral amplitude

Introduction

Plavinu HPP is the largest hydroelectric power plant in the East Baltic region. The station's electrical capacity is 894 MW per year. The station was built in the mid-60s of the 20th century. 20 years later, in 1986, as a result of seismic exploration in the area of the Plavinu HPP, *Piebalga* and *Aizkraukle* tectonic faults were identified in the crystalline basement and the Caledonian structural complex of the sedimentary cover (Fig. 1). Quaternary deposits are located in the upper part of the sedimentary cover. They consist of loose deposits of sand, sandy loam, loam, gravel, pebbles, and boulders located on Devonian deposits, represented by sandstones, dolomites, marls, and other rocks.

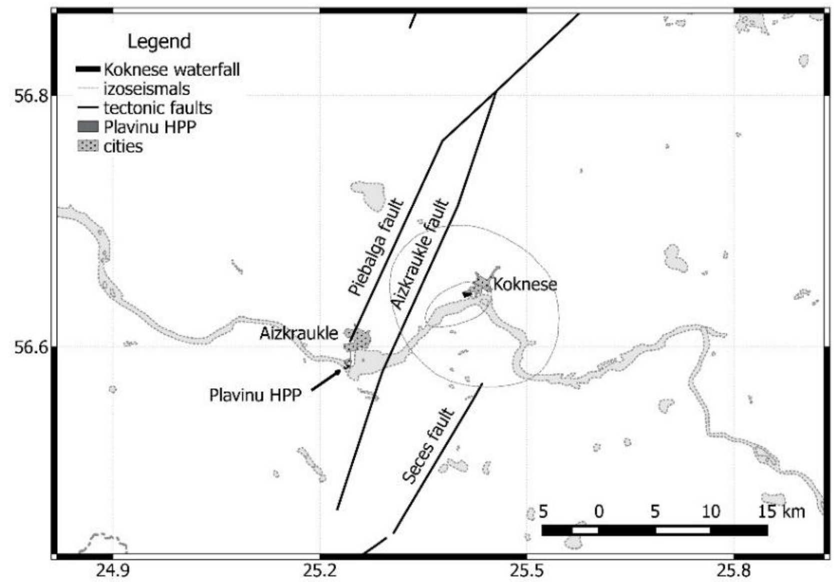

Fig. 1. Map of the location of the Plavinu hydroelectric power plant, the seismic source in *Koknese*, tectonic faults and isoseisms [Doss, 1909] of the 1821 earthquake.

There is a significant difference in seismic stiffness between Quaternary and Devonian deposits, i.e. the product of the velocity of propagation of S-waves and the density of geological sediments. Geological conditions characterized by high seismic rigidity of Devonian deposits, which is favorable for the occurrence of resonance effects in the upper layer of soil. Resonance effects can cause increased vibrations of the ground and hydroelectric power station structures located on it. Plavinu HPP is located in the valley of the Daugava River. Erosion processes of the bank and riverbed, karst, suffusion, and slope processes are observed on the outer edges of the bends of the Daugava River, below the HPP. Slope processes (landslides) occur on both banks of the Daugava, not far from the HPP. These processes affect the stability of the soil.

A number of studies carried out at the HPP and in its vicinity revealed the existence of zones decompaction and also zones fracturing in the sedimentary cover in the upstream [Fugro, 2014] and downstream [Fugro, 2015], uneven deformation of the reinforced concrete slab [AS Latenergo, 2014] located under the HPP and complex geodynamic situation [Nikulins, 2019].

The mechanical impact of natural or man-made regional seismic sources can affect soils, increasing their resonance effect. It occurs when the thickness of a loose layer located on a rocky base is comparable to 1/4 of the seismic wavelength. Thus, knowledge of the wave field from regional seismic sources makes it possible to estimate the amplification of vibrations of the loose soil layer.

The territory of Latvia belongs to zones of low seismic activity [Nikulins, 2011]. Most historical earthquakes are known [Doss, 1909], which occurred in the East Baltic region before the beginning of the instrumental observation period, i.e., approximately until the mid-60s of the 20th century.

Among the earthquakes before the instrumental period were the *Koknese* earthquakes. From February 20 to February 23, 1821, several shocks occurred there (up to 7 shocks). The epicenters of these earthquakes are located in close proximity, 12.5 km, from the site of the Plavinu HPP. These earthquakes were studied by professor Bruno Doss, who published a catalog and map of earthquakes in the East Baltic Province [Doss, 1909], as well as an isoseismal map of earthquakes in *Koknese* (Fig. 2). In particular, the intensity of the strongest shock on 02/23/1821 was assessed to VIII points on the Rossi-Forel scale, the range of which is from I to X points.

More recent studies have made new estimates of shaking intensity. Thus, in 1988, the intensity of the main shock in *Koknese* was estimated at VI–VII points (MSK-64) [Avotinya et al., 1988], and in studies of 1995, the intensity of the shaking was estimated at VII points, magnitude 4.5 and focal depth 13 km (MSK-64) [Boborykin et al., 1995].

There is a point of view according to which some historical earthquakes on the East European Platform should belong to the class of non-tectonic earthquakes caused by landslides, karst sinkholes, and frost-quakes phenomena. The *Koknese* earthquakes of 1821 were classified as frost quakes (cryoseisms) [Nikonov, 2010].

However, according to the Institute of Seismology of the University of Helsinki, this earthquake is included in the Catalog of earthquakes in Northern Europe [FENCAT, 1375-2014]. This earthquake's intensity at the epicenter is VII points, a focal depth of 0 km, and a magnitude of 2.5 (FENCAT, 2014 https://www.seismo.helsinki.fi/bulletin/list/catalog/Scandia_updated.html).

The maximum radius of perceptibility of the earthquake of 1821 reaches 8.0–9.5 km. The optimal intensity of shaking was taken as VI points (MSK-64) at the epicenter, as was indicated in the 1988 studies [Avotinya et al., 1988].

According to the assessment of seismic hazard in Latvia [Nikulins, 2011], with a probability of 10 % within 50 years, an earthquake with an intensity exceeding 10 cm/s^2 on hard ground may occur in the area of *Aizkraukle* (the closest city to the Plavinu HPP). Therefore, the assessment of the soil response at the Plavinu HPP site seems relevant and important.

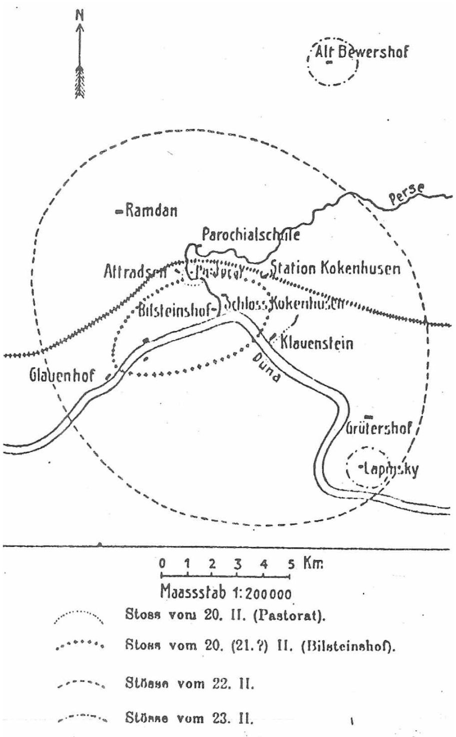

Fig. 2. Isoseismals map of the *Koknese* earthquakes of 1821 according to Bruno Doss [Doss, 1909]. (The old name of *Koknese* on the map is *Kokenhusen*).

The main goal of the research is to assess the wave field from the seismic source of 1821 in *Koknese* and to conduct the subsequent evaluation of ground motion parameters at the Plavinu HPP site. These assessments make it possible to identify the most vulnerable soil sites at the Plavinu HPP area.

A waterfall on the *Perses* River is at the epicenter of the main shock. The waterfall represents an almost vertical displacement in the rocky ground, with an amplitude of 2.5–3.0 m (Fig. 3). The waterfall is located near the village of *Bilsteinshof* (modern name *Bilstiņi*) (Fig. 1). After the Plavinu reservoir was filled, the waterfall was under water. The strike azimuth of the waterfall is approximately 74º.

Fig. 3. Waterfall on the *Perses* River (1920–1930).

For the isoseismal of the shock of February 20, 1821 (in Fig. 2 there is a smaller ellipse), the azimuth of the major axis of the ellipse is approximately 65º. The proximity of these azimuths indicates that the waterfall, on the *Perses* River, may have been the source of the 1821 earthquakes. The main shock occurred on February 23, 1821. The total perceptibility area of the earthquake of February 23, 1821 (large ellipse) is approximately 186 km^2.

Body wave magnitude mb estimates, in the range $2.7 \le mb \le 5.5$, are based on the equation for the central United States located on the North American Plate (Nutti & Zollweg, 1974):

$$mb = 2.65 + 0.098 \log A_f + 0.054(\log A_f)^2, \quad (1)$$

where, A_f – perceptibility area in km^2.

To estimate other types of magnitudes, we used the relationships for the Baltic region obtained as part of the 2008 seismic hazard assessment project in Latvia [Nikulin, 2007]:

$$M_w = 0.926mb + 0.679. \quad (2)$$

$$M_w = 0.7285M_s + 1.7854. \quad (3)$$

The depth of the hypocenter is estimated based on the macroseismic field equation for the Baltic region [Nikonov at al., 2007]:

$$I_o = 1.36M_s - 2.7\lg(h) + 3.36, \quad (4)$$

where I_0 – intensity at the epicenter, h – focal depth, km.

As a result, we got mb = 3.15 ~ 3.2, M_w = 3.6, M_S = 2.5, h = 1.9 km. The moment magnitude and focal depth will be used to calculate the wave field at the Plavinu HPP site.

Methods

The study of seismic impacts at the Plavinu HPP site from a seismic source in *Koknese* consisted of two separate and independent stages: 1) modeling of a synthetic wave field based on Green's functions; 2) modeling of the soil response to these seismic impacts.

Synthetic wavefield modeling

Green's functions were used to simulate the synthetic wave field. Green's functions are the impulse response of an inhomogeneous linear differential operator.

The propagation of a seismic wavefield in the time domain can be represented as a simple three-dimensional acoustic wave equation [Liu et al., 2021]:

$$\nabla^2 u(x,y,z,t) = \frac{1}{\nu(x,y,z)^2}\frac{\partial^2 u(x,y,z,t)}{\partial t^2} + f(x,y,z,t), \quad (5)$$

where ∇^2 – Laplace operator, $u(x,y,z,t)$, $v(x,y,z,t)$, $f(x,y,z,t)$ represent displacement, velocity, and source term, respectively. $f(x,y,z,t) = -\delta(x - x_s, y - y_s, z - z_s)s(t)$, $s(t)$ – the wavelet (in this case *Ricker* wavelet), $\delta(x - x_s, y - y_s, z - z_s)$ – the Dirac function at the source point (x_s, y_s, z_s).

After the Fourier transformation of equation (5), we obtain a two-dimensional equation of an acoustic wave in the frequency domain, after which the Green's function is determined by the following equation:

$$\nabla^2 G(x,y,z,w) + k^2 G(x,y,z,w) = F(x,y,z,w) \quad (6)$$

where G – Green's function, $F(x, y, z, w) = -\delta(x - x_s, y - y_s, z - z_s)s(w)$ – the source term in the frequently domain, $k(x, y, z) = w/v$ – wave number, $s(w)$ – Ricker wavelet in the frequency domain, w – angular frequency.

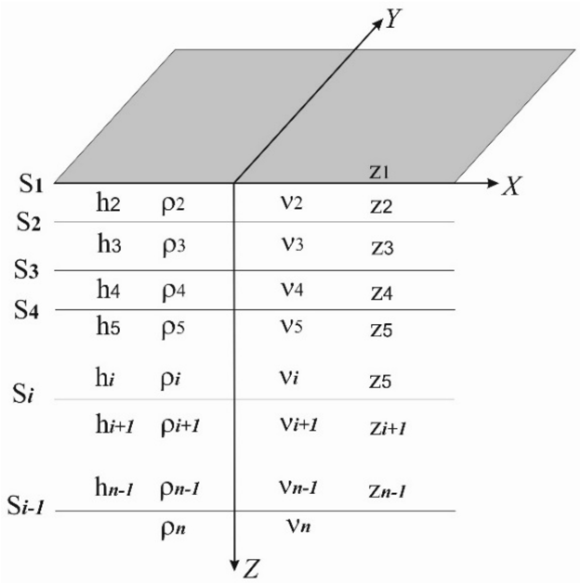

Fig. 4. The structure of a layered geological environment.

The geological medium has a certain viscosity, which leads to loss of wave energy and phase changes during wave propagation. To better describe the propagation of seismic waves in a viscous medium, complex velocity can be introduced into equation (6).

Since the modeling of the synthetic wave field took place in a multilayer medium, let us consider the layered symmetrical structure of a homogeneous geological medium, for which the interfaces are defined, located at points $z_1, z_2, \ldots, z_{n-1}$, as shown in Fig. 4. The density of each layer corresponds $\rho_1, \rho_2, \ldots, \rho_n$, and velocity – $v_1, v_2, \ldots, v_n$.

Each layer satisfies equation (6) with the parameters Green function G, wavenumber k, velocity v, density ρ, layer thickness h and quality factor Q, respectively. We get the equations in the following form:

$$\nabla^2 G_j + k_j{}^2 G_j = 0 \quad (i = 1,3,\ldots,n), \qquad (7)$$

$$\nabla^2 G_j + k_j{}^2 G_j = -S(\omega)\delta(R - R_o), (i = 2), \qquad (8)$$

where, $k_i = \dfrac{\omega}{\upsilon_i}\left(1 - \dfrac{j}{2Q}\right),\ j = \sqrt{-1}$.

At the interface, the pressure $P_i = \rho_i C_i$ as well as the gradient of the potential for the vertical direction $\partial G_i/\partial z_i$ are continuous. Therefore, the following boundary conditions can be imposed on the Green function:

$$\frac{\partial G_i}{\partial z} = \frac{\partial G_{i+1}}{\partial z}, \rho_i G_i = \rho_{i+1} G_{i+1}, (i = 1,2,\ldots,n-1). \qquad (9)$$

The solution to equations (7) and (8) can be regarded as the summation of separate reflected and refracted waves. Therefore, it can be written as the form of Sommerfeld integral in a cylindrical coordinate system [Liu et al., 2021]:

$$G_i = \frac{S(\omega)}{4\pi}\int_0^{\infty}(C_i e^{m_i z} + D_i e^{-m_i z}) J_0(mr)\,dm, (i = 1,3,\ldots,n), \qquad (10)$$

$$G_i = \frac{S(\omega)}{4\pi}\left[\frac{e^{-ik_i R}}{R} + \int_0^{\infty}(C_i e^{m_i z} + D_i e^{-m_i z}) J_0(mr)\,dm\right], (i = 2), \qquad (11)$$

where $m_i = \sqrt{m^2 - k_i^2}, k_i^2 = \dfrac{\omega^2}{\upsilon_i^2}, \upsilon_i = \nu_i\left(1 - \dfrac{j}{2Q_n}\right), i = 1,2,\ldots,n, j = \sqrt{-1}$, $J_0(mr)$ are the Bessel functions.

In equations (10) and (11), the terms $e^{m_i z}$ and $e^{-m_i z}$ may be infinity. To maintain numerical stability, rewrite them in the form:

$$G_i = \frac{S(\omega)}{4\pi}\int_0^{\infty}(C_i e^{m_i(z - z_i)} + D_i e^{-m_i(z - z_{i-1})}) J_0(mr)\,dm, (i = 1,3,\ldots,n), \qquad (12)$$

$$G_i = \frac{S(\omega)}{4\pi}\left[\frac{e^{-ik_i R}}{R} + \int_0^{\infty}(C_i e^{m_i(z - z_i)} + D_i e^{-m_i(z - z_{i-1})}) J_0(mr)\,dm\right], (i = 2). \qquad (13)$$

Using boundary conditions (9), the unknown $C_1, C_2, D_2, \ldots, C_i, D_i, \ldots, C_{n-1}, D_{n-1}, D_n$ in above formula are solved. Also, other coefficients can be obtained by recursion.

Synthetic wavefield modeling was performed using Computer Programs in Seismology [Hermann, 2002]. The seismic velocity model, source and receiver depth data, and epicentral distance were used as initial data. The modeling process consisted of separate software blocks. During the processing, additional input parameters were specified: frequency range for filtering, moment magnitude, azimuth from the source to the receiving point and back, parameters of the earthquake source mechanism. The intermediate result is the generation of 15 Green’s functions. The final result is a three-component accelerogram.

Soil response modeling

The simplest model for simulating the stress-strain state of soil under seismic impact is the viscoelastic

Kelvin–Voigt model. Of primary importance is the shear stress τ, which depends on the shear strain γ and strain rate $\dot{\gamma}$ as follows [Bardet & Tobita, 2001]:

$$\tau = G\gamma + \eta\dot{\gamma}, \qquad (14)$$

where G – shear modulus, η – viscosity.

In the case of a harmonic load with a circular frequency ω, equation (18) takes the form [Bardet & Tobita, 2001]:

$$\tau(t) = \Sigma e^{i\omega t} = (G + i\omega\eta)\Gamma e^{i\omega t} = G^{*}\gamma(t), \qquad (15)$$

where G^{*} – complex shear modulus, Σ – amplitude of shear stress, Γ – amplitude of shear strain.

Considering the critical damping coefficient $\xi = \omega\eta/2G$, the complex shear modulus G^{*} takes the form:

$$G^{*} = G + i\omega\eta = G(1 + 2i\xi). \qquad (16)$$

The linear approach in the Kelvin-Voigt model considers some types of soil nonlinearity, expressed in the form of hysteretic deformation of soil behavior under cyclic loads.

The Iwan [Iwan, 1967] and Mroz [Mroz, 1967] model considers nonlinear stress-strain curves using n mechanical elements having different stiffness k_i and sliding resistance Ri. In the case of one-dimensional soil response analysis, shear waves propagate vertically in the layered system (Fig. 5).

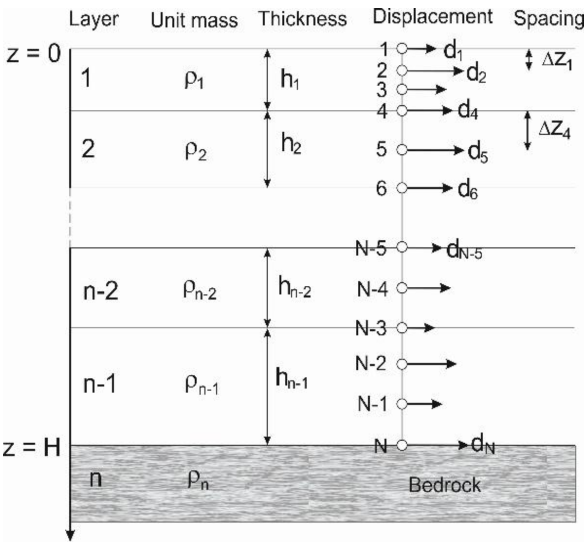

Fig. 5. One-dimensional, layered sedimentary system and its spatial discretization.

It is assumed that the soil layers are oriented horizontally and have an infinite extent. They are only subject to horizontal movement from the bedrock.

The basic equation in this case is [Bardet & Tobita, 2001]:

$$\rho\frac{\partial^2 d}{\partial t^2} + \eta\frac{\partial d}{\partial t} = \frac{\partial\tau}{\partial z}, \qquad (17)$$

where ρ – soil unit mass, d – horizontal displacement, z – depth, t – time, τ – shear stress, η – mass-proportional damping coefficient.

Boundary conditions defined at the free surface (z – 0) and at the bottom of the sediment column (z – H): $\tau = 0$ for $z – 0$, and $\tau = \tau_B$ for $z = H$. The shear stress τ_B, which is usually unknown, is calculated from the velocity for z = H.

Soil response calculations were performed using NERA – Nonlinear Earthquake Site Response Analysis of Layered Soil Deposits [Bardet & Tobita, 2001]. A parametric velocity model and an input signal (accelerogram) were used as input data. During the processing, the deformation, the input velocity according to the given acceleration and the predicted velocity were calculated, and the increment of deformation and stress was estimated. The end results were Amplification, Fourier amplitude and Spectral amplitude.

Results

Synthetic wavefield modeling

In the synthetic wavefield simulation, intermediate results were first obtained that included a complete specification of the ray propagation between source and receiver. After leaving the source, the ray can be directed up or down. Further, the ray can interact with the adjacent boundary, also directed either up or down. The entire variety of reflected and refracted rays is shown in Fig. 6.

The earthquake source (SRC) and receiver (REC) are located in layers 2 and 1, respectively. The five-layer model includes 4 layers of the earth's crust and the last layer is the upper mantle. The receiver depth (REC = 0.01 km) corresponds to the depth of the Devonian surface on which Quaternary deposits are located. This is due to the fact that at the next stage the "input" signal will act specifically on the Devonian surface.

The selection of the initial pulse is an important stage in wave field modeling. For this purpose, an optimal parabolic pulse with a duration of 2 seconds was chosen. Next, the functional description of each ray was convolved with the second derivative of the original time function, as a result of which 15 Green's functions were generated and synthetic seismograms were created (Fig. 7). Green's functions include the following components: ZDD, RDD, ZDS, RDS, TDS, ZSS, RSS, TSS, ZEX, REX, ZVF, RVF, ZHF, RHF, THF. These functions have the following meaning: ZDD – Vertical Component 45º dip slip; RDD – Radial Component 45º dip slip; ZDS – Vertical Component 90º dip slip; RDS – Radial Component 90º dip slip; TDS – Tangencial Component 90º dip slip; ZSS – Vertical Component vertical strike-slip; RSS – Radial

Component vertical strike-slip; TSS – Tangencial Component vertical strike-slip; ZEX – Vertical Component Explosion; REX – Radial Component Explosion; ZVF – Vertical Component Downward Vertical Force; RVF – Radial Component Downward Vertical Force; ZHF – Vertical Component Horizontal Force; RHF – Radial Component Horizontal Force; THF – Tangential Component Horizontal Force.

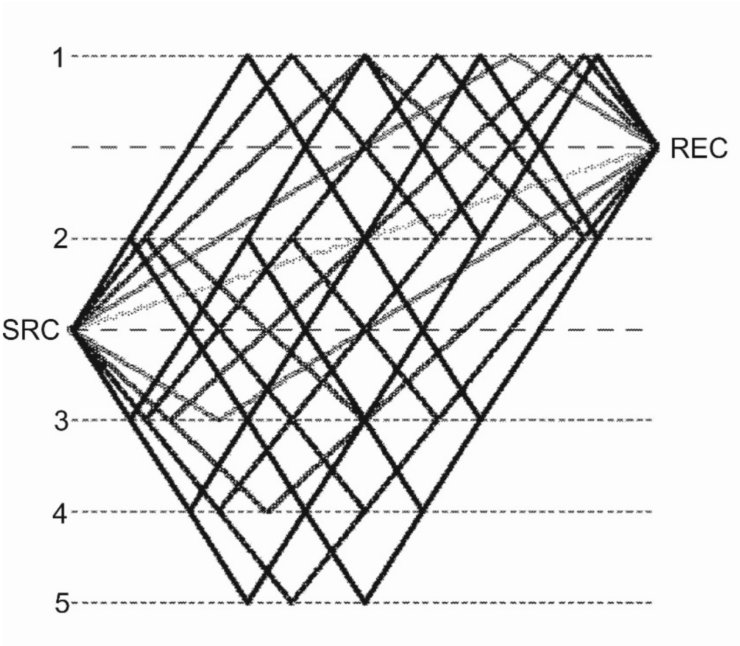

H, km	Vp, km/s	Vs, km/s	ρ, g/cm³
1	2.60	1.50	2.32
29	6.25	3.59	2.78
10	6.85	3.94	2.91
8	7.45	4.28	3.07
	8.00	4.60	3.20

Fig. 6. Ray propagation diagram between source (SRC) and receiver (REC), and velocity model in the earth's crust.

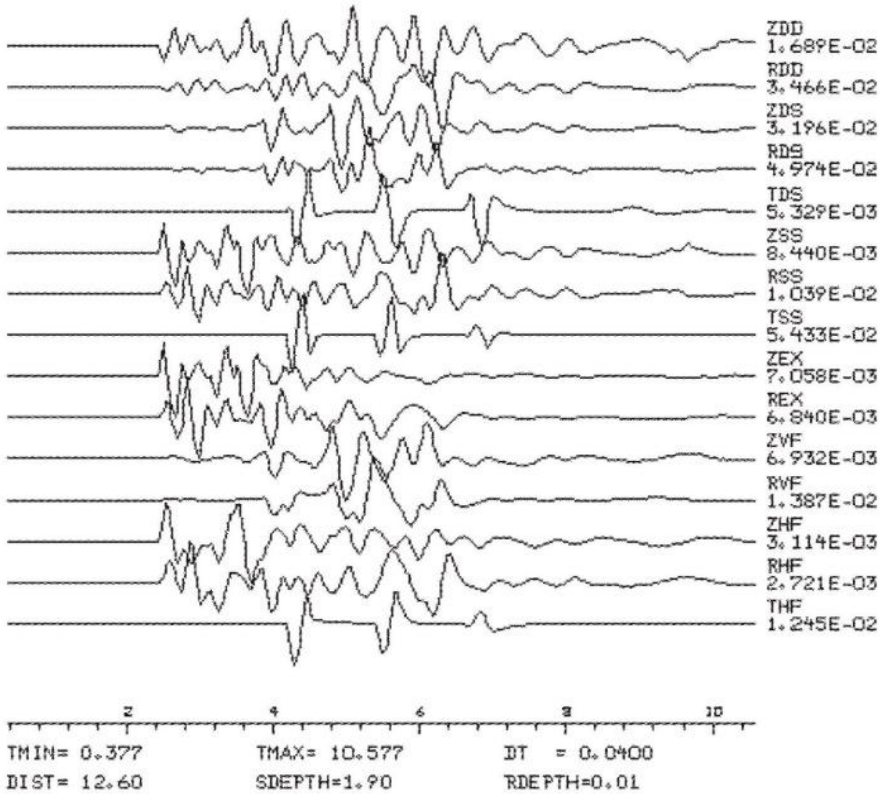

Fig. 7. Green's functions:
TMIN and TMAX – seismic record reproduction limits, DT – sampling step, DIST – distance between source and receiver, SDEPTH – source depth, RDEPTH – "receiver" depth (Devonian surface).

The frequency range for the regional earthquake was selected in the range from 0.5 to 10 Hz. For this purpose, filtering was applied using a 3rd order Butterworth filter. In addition, the optimal parameters of the earthquake source were used: DIP = 85º, STRIKE = 75º, RAKE = 135º. Thus, proposed source mechanism of the *Koknese* earthquake in 1821 was chosen as a reverse right-lateral oblique (Fig. 8).

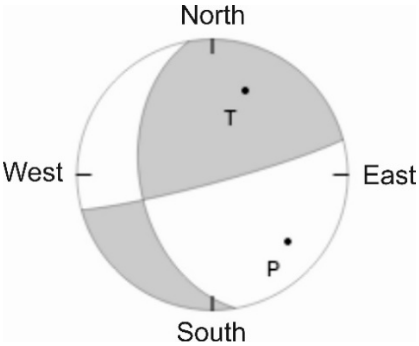

Fig. 8. Proposed source mechanism of the *Koknese* earthquake in 1821.

For the given parameters of the earthquake source mechanism, the azimuth of the maximum horizontal compression is 131.2º, and the dip angle is 25.9º.

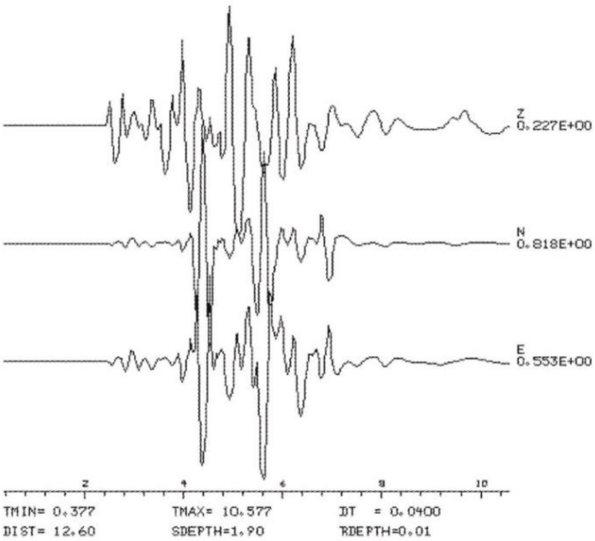

Fig. 9. Three-component accelerogram at the Plavinu hydroelectric power plant site from a seismic source in *Koknese* (Latvia).

The choice of these parameters is determined by the following arguments: the waterfall plane (DIP) is oriented almost vertically, the strike azimuth (STRIKE) is known and corresponds to the strike azimuth of the waterfall, the sliding direction (RAKE) in the fault plane refers to the optimal azimuth of the maximum horizontal stress in the East Baltic region. The azimuth of the maximum horizontal stress was estimated as the average value between the same azimuths of the maximum horizontal stress for the Kaliningrad earthquakes of September 21, 2004 [Gregersen et al., 2007] and the Estonian earthquakes for the period from 1976 to 2018 [Soosalu et al., 2022].

At the final stage of modeling the synthetic wave field, a 3-component accelerogram was obtained (Fig. 9). Ground acceleration is expressed in cm/s^2.

The designations are similar to those in Fig. 7.

Soil response modeling

Modeling of soil reaction was carried out for the site upstream of the Plavinu HPP dam. In this site, the geological section is represented by a 3-layer model, consisting of two layers of Quaternary sediments located on the surface of Devonian sediments, represented by dolomite.

The process of modeling the soil response included several intermediate stages. These are 1) reading the initial accelerogram data (the result obtained at the first stage of research) for a given component (Z, N, E); 2) generating a parametric section using various parameters (shear modulus, damping coefficient) from the data set; 3) calculation maximum shear strain and stress, as well as maximum acceleration and velocity depending on depth; 4) calculation of displacement, velocity, and acceleration at the surface and at the base (in this study – the surface of Devonian sediments); 5) calculation of deformation, stress, strain energy and relationships between stress and strain on the surface.

The main results of soil response modeling are 1) surface amplification; 2) Fourier amplitudes;3) spectral acceleration. All main results of soil response modeling are shown in Fig. 10 and are presented in Table.

The increase in ground vibrations on the surface gives a clear idea of the intensity of vibration and the vulnerability of a particular site of the Plavinu HPP when exposed to a seismic signal or vibration with a predominant frequency of 8 Hz. For all three components the gain is the same and equals 2.6.

Main results of soil response modeling at the Plavinu HPP site (upstream)

Component	Amplification Frequency (Hz)	Fourier amplitudes (g) Frequency (Hz)	Spectral amplitudes (g) Period (sec)
Z	2.59 8.0	0.00042 2.07	0.0055 0.33
N	2.59 8.0	0.00028 3.31	0.0046 0.31
E	2.59 8.05	0.00024 2.51	0.0037 0.24

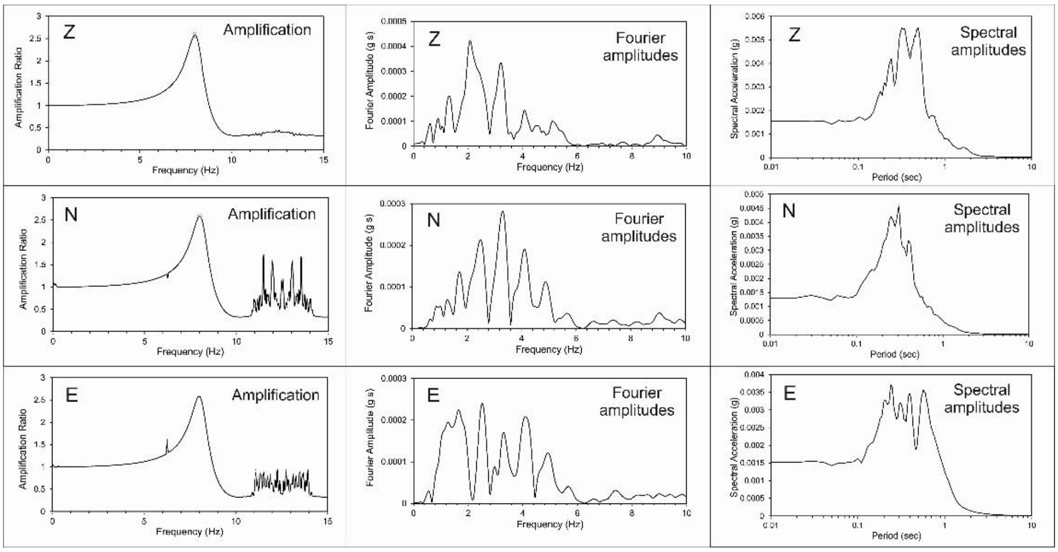

Fig. 10. Results of modeling the soil reaction in the upper reaches of the Plavinu HPP from a seismic source located in *Koknese*.

Fourier amplitudes provide important information about the frequency content of a signal and can be used for signal processing and analysis. Spectral amplitudes are of greater practical importance, since they can be used for the purposes of engineering seismology.

This study demonstrates the practical feasibility of using macroseismic data on historical seismic events for wave field modeling. This method is especially relevant for intraplate areas, where earthquakes rarely occur and therefore, any information, including the one about historical seismic events, is important.

The practical significance of the research lies in the possibility of assessing the response of the soil in different sites of an engineering facility using a synthetic seismogram from a regional seismic source. Such assessments make it possible to identify vulnerable sites of soil in these areas and predict the engineering and seismic characteristics of the soil when certain background parameters change (for example, when the groundwater level changes).

Conclusions

As a result of modeling synthetic seismograms, a wave field was obtained at the Plavinu hydroelectric power plant from a regional seismic source of natural origin located in the *Koknese* region. The implementation of this task is based on the use of macroseismic data from the historical earthquake of 1821.

For three components Z, N, E, the study assessed the predicted impacts on the ground surface in one of the sites of upstream of the Plavinu HPP: 1) amplification of oscillations relative to the base of the rocky soil; 2) Fourier amplitudes and 3) spectral amplitudes.

The seismic characteristics of the soil may change with changes in geological, hydrogeological, and geodynamic conditions in the area of the Plavinu HPP. In the area surrounding the Plavinu HPP, there is a risk of the earth's crust subsiding in separate areas and changes in the water saturation of soils. These factors, known as geodynamic and hydrogeological factors respectively, can increase the likelihood of natural hazards. Therefore, it is of utmost importance to assess the engineering and seismic characteristics of the area and take preventive measures to reduce the consequences of these risks.

To monitor changes in seismic-geological and geodynamic conditions in the area of the Plavinu HPP, it is advisable to organize seismic observations. Seismic monitoring can help in solving geodynamic problems such as monitoring fast movements, including earthquakes and quarry blasts, as well as slower movements, e.g. tectonic creep. It can also provide systematic monitoring of the stability of soil parameters.

References

AS Latenergo (2014). Plavinu HES hidrotehnisko buvju drosuma deklaracija. Parskats par HES hidrotehnisko buvju drosuma programmas izpildi laikposma no 2013.g.1.janvara lidz 2013.g.31.decembrim. Author: Z. Zegele (In Latvian).

Avotinya I. Ya., Boborykin A. M. et al (1988). Catalog of historical earthquakes in Belarus and the Baltic states. *Seismological bulletin of seismic stations “Minsk” (Pleschenitsy) and “Naroch” for 1984*, 126–137 (In Russian).

Bardet J. P., Tobita T. (2001). NERA. A Computer Program for Nonlinear Earthquake site Response Analyses of Layered Soil Deposits. 44 p.

Boborykin et al. (1995). Seismotectonic studies of the west of the East European Platform (Belarusian-Baltic region). *Seismological Research*, 2, 5–54 (In Russian).

Doss B. (1909). Die historish beglaubigten Einsturzbeben und seismish-akustishen phonomene der russischen Ostseeprovinzen. Beitrage tuz Geophysik. Leipzig, B.X, H.1, 1–124 (In German).

FENCAT. Catalog of earthquakes in North Europe 1375–2014. https://www.seismo.helsinki.fi/bulletin/list/catalog/Scandia_updated.html

Fugro Consult GmbH. (2015). Report. Geophysical investigation from the right bank boreholes at Plavinas HPP and in the horizontal profiles of the area next to the powerhouse. Abteilung Geophysik Suptitzer Weg 28 A, DE-04860 Torgau. Author: F.Meier.

Fugro Consult GmbH. (2014). Investigation Works in the Plavinas HPP, 2014. Abteilung Geophysik Suptitzer Weg 28 A, DE-04860 Torgau. Author: C. Richter.

Gregersen S., Wiejacz P., Debski W. et al. (2007). The exceptional earthquakes in Kaliningrad district, Russia on September 21, 2004. *Physics of Earth and Planetary Interior*, 164, 63–74.

Hermann R. B. (2002). Computer Programs in Seismology. An overview of synthetic seismogram computation.

Iwan W. D. (1967). On a class of models for the yielding behavior of continuous and composite systems. *Journal of Applied Mechanics*, ASME, 34, 612–617.

Liu S., Zhou Z., Dai S. Et al. (2021). Fast Computation of Green Function for Layered Seismic Field via Discrete Complex Image Method and Double Exponential Rules. *Symmetry*, 13, 1–12. https://doi.org/10.3390/sym13101969

Mroz Z. (1967). On the description of anisotropic workhardening. *Journal of Mechanics and Physics of Solids*, 15, 163–175.

Nikonov A. A., Pačesa A., Aptikaev F. F., Nikulin V. G., Puura V., Aronov A. G. (2007). Kaliningrad, September 21, 2004, Earthquake in the East Baltic area – basic macroseismic maps for three main shocks. Seismicity and seismological observations of the Baltic region and adjacent terrirories. Volume of abstracts. 60–62.

Nikonov A. A. (2010). Frost shaking as a special class of seismic phenomena (based on materials from the East European Platform). *Physics of the Earth*, 3, 79–96 (In Russian).

Nikulins V. (2007). An overview of the results of the work, the assessment of the seismic impact on the buildings and the conditions on the building, in accordance with the requirements of Eurostandard 8, the preparation of the national annex project LVS EN 1998-1:2005 and proposals for amendments to the building standard LBN-005-01 “Engineering rules for construction” (In Latvian).

Nikulin V. (2011). Assessment of the seismic hazard in Latvia. Version of 2007 year. *Material Science and Applied Chemistry*, 1, 24, 110–115.

Nikulins V. (2019). Geodynamic Hazard Factors of Latvia: Experimental Data and Computational Analysis, *Baltic Journal Modern Computing*, 7 (1), 151–170. https://doi.org/10.22364/bjmc.2019.7.1.11

Nutti O. W., Zollweg J. E. (1974). The Ralation Between Felt Area and Magnitude for Central United States Earthquakes. *Bulletin of Seismological Society of America*, 64, 73–85.

Soosalu H., Uski M., Komminaho K., Veski A. (2022). Recent Intraplate seismicity in Estonia, East European Platform. *Seismological Research Letter*, XX, 1–12.

Валерій НІКУЛІНС[1], Дмитро МАЛИЦЬКИЙ[2]

[1] SIA Geo Consultants, Olivu iela 9, Riga, LV-1004, Латвія, e-mail: seismolat@gmail.com, https://orcid.org/0000-0003-4489-8708
[2] Карпатське відділення Інституту геофізики імені Субботіна НАН України, e-mail: dmalytskyy@gmail.com, https://orcid.org/0000-0002-9156-739X

ПРОГНОЗ СЕЙСМІЧНИХ ВПЛИВІВ НА ДІЛЯНЦІ ПЛАВИНСЬКОЇ ГЕС ВІД ПОТЕНЦІЙНОГО СЕЙСМІЧНОГО ДЖЕРЕЛА В КОКНЕСЕ (ЛАТВІЯ)

Розглянуто вплив сейсмічних хвиль від джерела потенційного землетрусу на ділянку Плавинської ГЕС у Латвії, яка розташована в несприятливих геологічних, тектонічних і геодинамічних умовах. Для оцінки сейсмічного впливу розв’язано пряму сейсмологічну задачу за два етапи. На першому етапі виконано моделювання синтетичних сейсмограм, а на другому – прогнозування сейсмічних впливів на майданчику ГЕС. На першому етапі використано моделювання хвильового поля із застосуванням методу Гріна. На другому етапі характеристики руху ґрунту визначено за допомогою одновимірного нелінійного аналізу відгуку ґрунту. Отримано хвильове поле з використанням 15 функцій Гріна, яке потім перетворено на трикомпонентну акселерограму. Після цього акселерограму використано як сейсмічний імпульс до поверхні дочетвертинних відкладень. Отримано комплекс інженерно-сейсмічних характеристик ґрунту: підсилення, амплітуди Фур’є та спектральні амплітуди. Продемонстровано можливість одержання важливої інформації про поле сейсмічних хвиль і рух ґрунту з макросейсмічних даних історичних землетрусів. Це особливо важливо для внутрішньоплитних умов з обмеженою сейсмічною статистикою. Оцінки інженерно-сейсмічних умов мають важливе практичне значення, оскільки дадуть змогу виявити найвразливіші ділянки ґрунту на Плавинській ГЕС.

Ключові слова: функції Гріна; синтетичне хвильове поле; відгук грунту; підсилення; амплітуда Фур’є; спектральна амплітуда.

Received 14.10.2023